Multi-Model Deep Learning Approach for Multi-Class Brain Tumor Detection from MRI

1st Abu Mukaddim Rahi
Electrical and Computer Engineering
North South University
Dhaka, Bangladesh
abu.rahi@northsouth.edu

2nd Mariam Binte Bashir
Electrical and Computer Engineering
North South University
Dhaka, Bangladesh
mariam.binte@northsouth.edu

3rd Maher Ali Rusho*
Dept. of Lockheed Martin
Engineering Management
University of Colorado, Boulder
Boulder, Colorado, USA
maher.rusho@colorado.edu

4th Md. Khurshid Jahan
Dept. of Electrical and Computer Engineering
North South University
Dhaka, Bangladesh
khurshid.jahan@northsouth.edu

***Abstract*—The classification of the diverse types of brain tumors is critical for automatically diagnosing the four classes, such as "glioma," "meningioma," "pituitary," and "no-tumor." Significantly, for the classification task, we employed custom light convolutional neural networks (CNNs) and optimized transformer-based models such as EfficientNetB0, EfficientNetB4, ResNet101, Xception, and Swin Transformer to compare their significance and accuracy. Moreover, advanced One-Hot Encoding, Adaptive Moment Estimation (Adam), and augmentation techniques have been used to enhance the potency and speculation of our system. Consequently, we achieved an accuracy of 99.08% on the custom light CNN and 99.61% on the EfficientNetB4, outperforming all other models. Our primary contributions include developing a lightweight custom CNN optimized for real-time deployment and integrating fine-tuned transformer models, achieving a best-in-class accuracy on MRI-based brain tumor classification. In addition, our selection of CNN for brain tumor classification was boosted by its assertive computational efficiency and significance in medical image research tasks. Subsequently, we used the Swin Transformer to improve quality extraction by catching both local and international contexts, which contributed to enhanced tumor localization and classification implementation.**

***Index Terms*—MRI images, CNN, classification, brain tumor, model, disease**

I. Introduction

The brain is a vital organ of the central nervous system (CNS) and is responsible for maintaining physical, mental, and emotional functions, and any abnormality in its design can have deep importance. Brain tumors represent a critical medical challenge, with 300,000 new cases identified globally each year [1]. Their complex nature and impact on essential brain functions pose significant health risks. However, imaging technologies such as MRI and CT scans play a key role in diagnosing and evaluating these tumors, allowing for early detection and follow-up, which are essential for adequate treatment [2]. Nevertheless, the central nervous system comprises intricate networks of neurons that connect the brain and spinal cord.

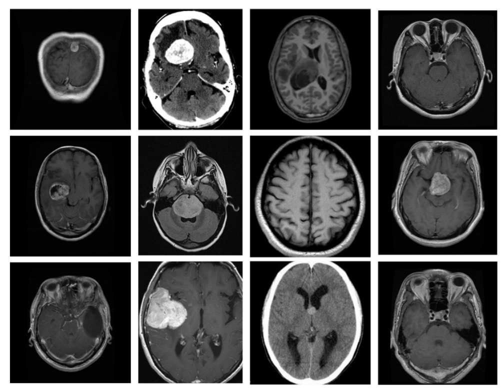

Fig. 1. Brain Tumor MRI image from the dataset

The most common symptoms include:

1) Continuous headaches – Often deteriorating in the morning or with physical activity, due to raised intracranial pressure [3].
2) Outbreaks – Unexplained seizures are a typical sign, especially in adults without a previous history.
3) Cognitive or natural changes – Including memory failure, confusion, or difficulty concentrating, which may result from tumor tension on distinct brain regions.
4) Eyesight or hearing issues – Such as blurred eyesight, double vision, or hearing failure, depending on the tumor's site.

A brain tumor diagnosis generally begins with neuroimaging methods such as magnetic resonance imaging (MRI) to detect irregularities within brain tissues [4].

In this study, we concentrate on categorizing brain tumors from MRI scans employing several deep learning architectures, including a lightweight custom CNN, EfficientNetB0, EfficientNetB4, ResNet101, Xception, and the Swin Transformer.

[5] [6] [7] [8] We employ a standardized multi-class MRI dataset, applying preprocessing and data augmentation to enhance the model arrangement. These models are trained to determine four tumor categories: glioma, meningioma, pituitary tumor, and no tumor. Each model is estimated using accuracy scores, loss values, and confusion matrices to pick the most effective solution. While deep models like Swin Transformer and EfficientNetB4 achieve advanced results, the custom CNN presents a computationally efficient alternative for real-time deployment. The key contributions of our proposed method:

- **Dual-Stream Hybrid Design:** The proposed system introduces a notable integrated lightweight custom CNN and fine-tuned transformer models, achieving both high accuracy and optimized computational expense.
- **Enhancing Accuracy:** High-resolution MRI data and one-hot encoded labels are used to classify four tumor types with minimal error. Augmentation, validation split, and regularization improve robustness, achieving up to 99.61% test accuracy.
- **Increasing Efficiency:** With reduced layers and computational cost, the lightweight custom CNN offers high implementation efficiency. To make the system suitable for real-time and boundary deployments, it allows fast training and lower memory usage in hypothesis.

The paper is structured as follows: Section 2 possesses the literature review. Section 3 summarizes the methodology, including the details of the lightweight custom CNN, fine-tuned backbone models, adaptive moment estimation (Adam), one-hot encoding, and the dataset. Section 4 illustrates the results and analysis, focusing on various preprocessing methods applied to the models and algorithms. Finally, Section 5 delivers future work and the conclusions, followed by the necessities.

II. Literature Review

Several analyses have been conducted in the field of brain tumor classification employing deep learning and conventional machine learning approaches. Xiaoyi Liu et al. [9], concentrate on indicating the type of brain tumors using four different types of MRI-based images. Moreover, they employed one unique model, that is MobileNet-BT. Similarly, Majid Behzadpour et al. [10], adopted EfficientNet to balance high accuracy with computational cost efficiency. They presented an intensive data augmentation pipeline to enhance representation. To detect intricate patterns within the BreakHis dataset, they fine-tuned the model using transfer learning. They achieved 98.23% accuracy for benign cases and 95.04% accuracy with transfer learning. Besides, Tina Dudeja et al. [11], proposed a neural model that enhances robustness by capturing images in three dimensions to extract features in the U-Net encoder. They achieved a mean accuracy of 99.24%. However, Arpita Ghosh et al. [12], offered a novel classification framework that includes pre-trained and fine-tuned EfficientNetB7. They focused on multi-class classification with the three common classes. They gained 99% test accuracy with the Nadam optimizer. Jainy Sachdeva et al. [13], employed principal component analysis for the removal of dimensionality of the feature length and classified by an artificial neural network phrase as the PCA-ANN approach. By their approach, they got an accuracy of 91% from 77%. For brain tumor detection, K. Nishanth Rao et al. [14], suggested the use of Convolutional Neural Networks. To categorize brain cancer cases, they pre-trained CNNs and applied data augmentation techniques. Also, they got the highest accuracy by operating ResNet50 and EfficientNet. Nonetheless, Mariam Binte Bashir et al. [15], submitted a custom lightweight convolutional neural network using the data-efficient image transformer (DeiT). They used ResNet50, InceptionV3, VGG16, and many more models. Among all the models, the custom lightweight CNN gained 99.71% accuracy. Besides, Neelum Noreen et al. [16], focused on various kinds of brain tumors. They utilized deep learning for the advancement of brain tumor classification. From the Inception-v3 model, they attained the highest accuracy of 94.34%, corresponding with additional recent methods.
In addition, ”Brain Tumor MRI Dataset” was employed for the precise identification of brain tumors, where Akmalbek Bobomirzaevich Abdusalomov et al. [17] introduced an improved variant of the YOLOv7 model within an enhanced detection framework, achieving 99.5% accuracy. In a similar effort using the same dataset, Md Ashik Khan et al. [18] attained an accuracy of 98.67% through a comparative evaluation involving a custom-designed CNN and pre-trained networks such as ResNet18 and VGG16 for classification purposes. Importantly, our proposed approach demonstrates higher overall accuracy in tumor recognition compared to these prior methods and existing research in brain tumor diagnostics.

III. PROPOSED SYSTEM

Our framework utilizes a dual-paradigm approach, combining a light CNN architecture with optimized transformer-based models to enhance brain tumor classification from MRI scans. The objective is to conceive a potent classification channel that accurately specifies tumor categories. Following several image pre-processing steps, the MRI image pieces are then packed from a Keras-compatible manual system. The dataset was sourced from Kaggle and was pre-divided into distinct training and testing sets. For acquiring the best accuracy, the system leverages the strengths of classical convolutional models and the power of advanced pre-trained models such as EfficientNetB0, EfficientNetB4, Swin Transformer, Xception, ResNet101, and Customized CNN. However, by utilizing different machine learning approaches, we fine-tuned diverse models for the classification of brain tumors into four different categories, which are: glioma, meningioma, pituitary, and no tumor.

A. Dataset

We used a brain MRI dataset shared on Kaggle, which combines data from three publicly known sources. The dataset contains a total of 7,023 MRI brain scan images, classified into four distinct categories: glioma, meningioma, pituitary tumor,

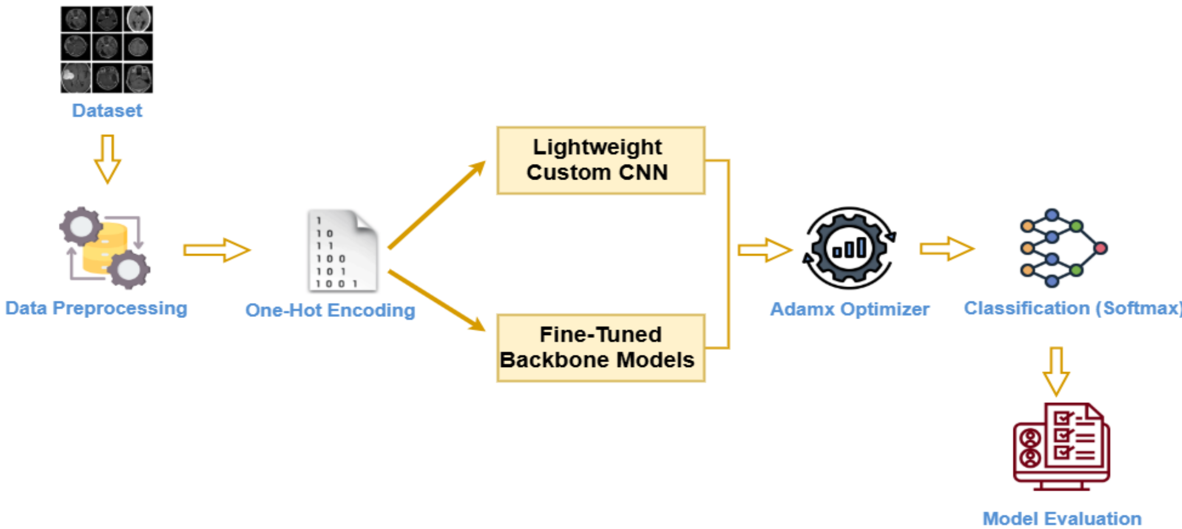

Fig. 2. Workflow of the proposed Brain Tumor Classification system

and no tumor. For the no-tumor class, images were collected from the Br35H dataset. while Figshare data was prioritized over SARTAJ due to labeling inconsistencies noted in the glioma category. The dataset contains both training and testing directories, with the test set retaining 1,311 images distributed across all four tumor classes. The images vary in dimensions and require preprocessing steps such as resizing and margin reduction to normalize input and improve model performance. All scans are in JPEG format, making them compatible with numerous image-based deep learning pipelines [19].

B. One-Hot Encoding

For brain tumor types, we employed one-hot encoding to represent the unconditional class labels. Our dataset consists of four distinct classes: glioma, meningioma, pituitary tumor, and no tumor. To make labels consistent with the multi-class classification structure, we applied one-hot encoding automatically through the ImageDataGenerator with the parameter class-mode = 'categorical'. This transforms each label into a binary vector where the indices of all other classes are set to 0, and the index of the actual class is set to 1. For training

TABLE I
ONE-HOT ENCODING FOR BRAIN TUMOR LABELS

Label	One-Hot Encoding
glioma	[1, 0, 0, 0]
meningioma	[0, 1, 0, 0]
no tumor	[0, 0, 1, 0]
pituitary	[0, 0, 0, 1]

the model using the categorical cross-entropy loss function, one-hot encoding is essential, as it ensures proper gradient flow and allows the model to learn accurate class probabilities [20]. Table I shows the one-hot encoding representation of the four brain tumor classes used for classification.

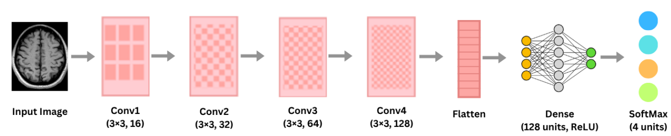

Fig. 3. Architecture Diagram for Lightweight Custom CNN

C. Lightweight Custom CNN

In this study, a lightweight, custom-designed CNN was developed to achieve high classification accuracy while maintaining low computational demands, making it suitable for deployment in clinical settings. The process of constructing the lightweight custom CNN is customized to 128×128×3 pixels, reducing input complexity while retaining critical diagnostic features. The network consists of four convolutional layers with progressively increasing filter sizes (Conv1: 16, Conv2: 32, Conv3: 64, Conv4: 128), each activated by ReLU functions to ensure effective feature extraction. Max-pooling layers are applied after selected convolutional layers to efficiently downsample the feature maps, minimizing computational load without sacrificing performance. A schematic representation of the lightweight custom CNN is provided in Figure 3.

Additionally, the network includes several convolutional layers, each employing ReLU activation to ensure robust feature extraction. Max-pooling is applied after specific convolutional blocks to reduce the spatial size of feature maps. Dropout is used after dense layers to minimize overfitting and improve model robustness. The architecture concludes with a final dense layer using softmax activation to produce class probabilities. As a result, this streamlined design successfully balances high accuracy with computational efficiency.

As shown in Figure 3, the CNN processes the input MRI image through four convolutional layers with increasing filter sizes. This design achieves a balance between accuracy and ef-

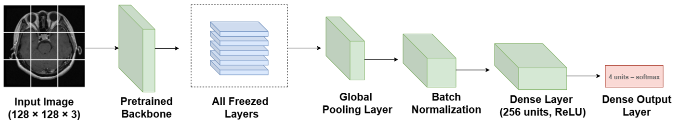

Fig. 4. Architecture Diagram for Fine-Tuned Backbone Models

ficiency, making it well-suited for real-time medical diagnostic applications.

D. Fine-Tuned Backbone Models

To enhance classification accuracy in brain tumor detection, multiple pre-trained models were fine-tuned and integrated into a hybrid system. For the image recognition task, architectures such as EfficientNetB0, EfficientNetB4, ResNet101, Xception, and Swin Transformer were utilized. These models were originally trained on the ImageNet dataset and subsequently adapted to our brain MRI data using transfer learning techniques.

To support reproducibility, a consistent fine-tuning strategy was applied with model-specific adjustments. For EfficientNetB0 and EfficientNetB4, all layers were frozen except the top 10. In ResNet101, the first 140 layers were frozen, while the final residual blocks were trainable. For Xception, the entry and middle flow blocks were frozen, and the exit flow was fine-tuned. In the Swin Transformer, the patch embedding and initial transformer stages were frozen, and the final stage and classification head were updated. Although a domain gap exists between natural images and medical images, freezing early layers is effective because they encode general low-level features like edges and textures, which remain relevant across domains. Additionally, given the limited size of medical datasets, freezing early layers reduces the risk of overfitting, lowers computational cost, and improves training stability.

To further enhance performance, a Batch Normalization layer was added after each backbone, followed by a Dense layer with 256 ReLU-activated units. This was regularized using L2 kernel regularization and L1 activity and bias regularization. A Dropout layer (rate: 0.45) was included before the final softmax layer to improve generalization. Figure 4 illustrates the shared architectural structure across all backbone models.

E. Adaptive Moment Estimation (Adam)

To train the lightweight custom CNN and the fine-tuned models, the Adamax optimizer, a category of the Adam optimizer, was utilized. Adamax is derived from the general Adam algorithm and is based on the infinity norm. It offers improved numerical stability during training, which is particularly beneficial for deep or fine-tuned architectures such as EfficientNetB4 and Swin Transformer. Adamax adapts the learning rate for each parameter individually by maintaining an exponentially decaying average of the first moment and

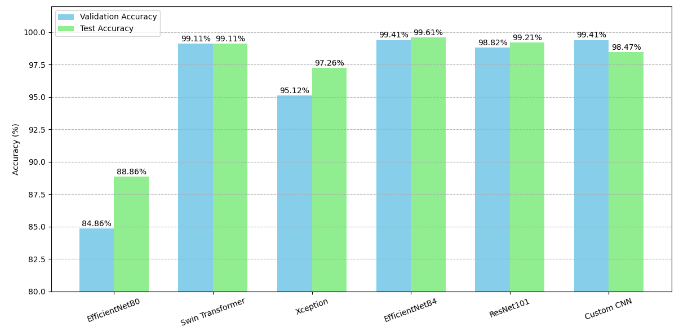

Fig. 5. Model-wise comparison of validation and test accuracy

the maximum absolute value of past gradients. The parameter update rule can be expressed as:

$$
\begin{aligned}
m_t &= \beta_1 m_{t-1} + (1-\beta_1) g_t, \\
u_t &= \max(\beta_2 u_{t-1}, |g_t|), \\
\theta_t &= \theta_{t-1} - \frac{\alpha}{1-\beta_1^t} \cdot \frac{m_t}{u_t}
\end{aligned}
$$

Where m_t is the first moment estimate (momentum term), u_t is the infinity norm-based scaling factor, and θ_t represents the updated parameters [5]. In this work, Adamax was employed with a learning rate of 0.001. It exhibited superior generalization performance compared to standard optimizers.

IV. RESULT AND ANALYSIS

A. Model Performance

We performed a comparative analysis to evaluate the robustness and inference capabilities of the proposed classification models based on validation and test accuracies across six deep learning architectures: EfficientNetB0, Swin Transformer, Xception, EfficientNetB4, ResNet101, and a custom lightweight CNN. The highest performance was recorded by EfficientNetB4, achieving an accuracy of 99.61%, closely followed by ResNet101 with 99.21%. The custom CNN attained a precision of 98.47%. Furthermore, the Swin Transformer achieved a peak validation accuracy of 99.11%. Similarly, EfficientNetB4 reached a test accuracy of 99.41%. The custom CNN achieved a high validation accuracy of 99.41%, based on a split of the original test set used during training monitoring, reflecting strong intermediate generalization. Contrarily, EfficientNetB0 exhibited the lowest validation and test accuracies, at 84.86% and 88.86% respectively, likely due to its comparatively lower representational capacity. Overall, the bar chart illustrates that although all models performed satisfactorily, the fine-tuned EfficientNetB4 and the custom lightweight CNN provided the most effective trade-off between accuracy and efficiency. Figure 5 presents a graphical comparison of the validation and test accuracies for all the evaluated models.

B. Performance Visualization

In Figure 6, the training and validation accuracy curves for both the Custom CNN and EfficientNetB4 models are presented. Figure 6(a) shows the performance of the lightweight

Custom CNN over 30 epochs. The model shows a sharp increase in training accuracy during early epochs, with the validation accuracy from a split of the test set following closely and peaking around epoch 13. The final performance is then evaluated at the last epoch. Similarly, the convergence of both curves reveals that the model generalizes to unrecognized data. Although small changes in validation accuracy are visible around the mid-training phase, they stabilize rapidly, suggesting minimal overfitting. Besides contributing to this stable and efficient learning behavior, the Custom CNN's surface architecture has been combined with regularization techniques such as dropout and batch normalization.

For instance, in Figure 6(b), the accuracy curve of the EfficientNetB4 model demonstrates an even faster conjunction, with training accuracy reaching above 99% by the 10th epoch. The validation accuracy continues to enhance steadily through 23 epochs, with the final accuracy also recorded at the last epoch. The smooth progression of the validation curve and its close alignment with the training curve emphasize the model's ability to fine-tune deep expressions effectively. Overall, both instances exhibit excellent training dynamics, with EfficientNetB4 achieving marginally higher performance, while the Custom CNN maintains a reasonable exchange between efficiency and accuracy. Figures 6(a) and 6(b) show the training and validation loss and accuracy for the Custom CNN and EfficientNetB4 respectively.

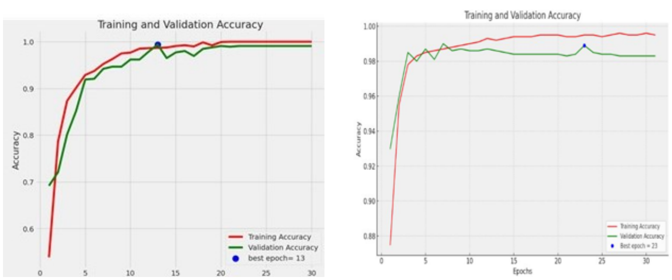

(a) (b)

Fig. 6. Training and validation accuracy curves

C. Classification Result

For glioma, it correctly classified 141; 140 instances were correctly classified for meningioma, 200 for no tumor, and 164 were pituitary instances, with only a few misclassifications. Contrarily, 8 glioma instances were confused with meningioma, and 1 meningioma instance was incorrectly predicted as glioma. This signifies that the model maintained high specificity and sensitivity across all four classes. Overall, the custom light CNN model functions very efficiently in our system. The confusion matrix for the Custom CNN is shown in Figure 7(a).

The EfficientNetB4 model demonstrated even stronger results, correctly classifying 161 glioma, 151 meningioma, 199 no tumor, and 141 pituitary instances. Minor errors included 6 glioma cases predicted as meningioma and 3 meningiomas as no tumor. Importantly, while both models performed well, per-class recall reveals critical insights for medical applications especially for tumor classes, where false negatives may delay diagnosis and risk patient safety. EfficientNetB4 showed strong classification performance for glioma and meningioma, with relatively few misclassifications. In contrast, the custom CNN, despite being lightweight, showed competitive recall and specificity, confirming its potential for real-time and resource-constrained deployments. Since false negatives carry more clinical risk than false positives, future evaluation should adopt cost-sensitive metrics that penalize missed tumor cases more heavily. These could include weighted loss functions or adjusted performance metrics.

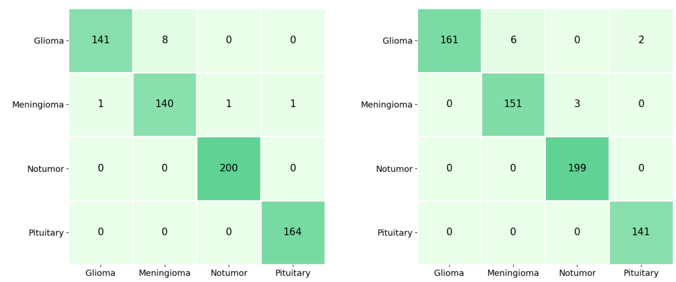

(a) (b)

Fig. 7. Confusion matrix for brain tumor classification

Significantly, almost all of the images were correctly classified as "glioma," "meningioma," "no tumor," and "pituitary," as shown in Figure 8. Notably, we used a custom Lightweight CNN model to classify the diseases.

D. Accuracy Comparison Table

Our system considers six deep learning architectures: EfficientNetB0, Swin Transformer, Custom CNN, EfficientNetB4, ResNet101, and Xception, trained and validated on a brain MRI dataset comprising four classes: "glioma," "meningioma,"

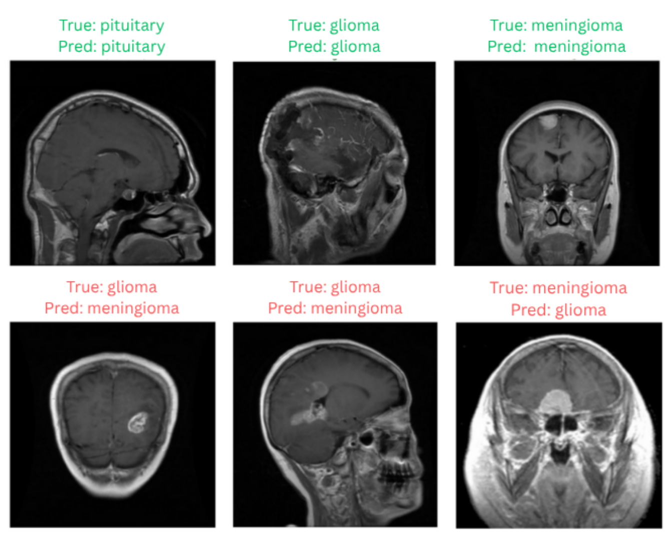

Fig. 8. Visual output of model predictions, highlighting both correct and incorrect classifications

"no tumor," and "pituitary." Among all models, EfficientNetB4 achieved the highest test accuracy of 99.61%, with a validation accuracy of 99.41% from a split of the original test set and the lowest test loss of 0.080, indicating excellent generalization and low error margins. Likewise, the Swin Transformer also performed competitively, achieving 99.11% accuracy on both validation and test sets, supported by low losses of 0.091 and 0.092, respectively. On the other hand, the custom light CNN, despite its lightweight design, showed remarkable results with 99.08% validation accuracy and 98.47% test accuracy. Again, ResNet101 showed robust performance with over 99% test accuracy, while Xception maintained a good balance with 95.12% validation and 97.26% test accuracy. Moreover, EfficientNetB0, the lightest variant of the EfficientNet family, recorded the lowest validation and test accuracy among all models, yet still maintained above 88% test performance.

TABLE II
VALIDATION AND TEST PERFORMANCE OF VARIOUS MODELS.

Model	Val Accuracy	Test Accuracy	Val Loss	Test Loss	Epochs
EfficientNetB0	84.86%	88.86%	0.387	0.420	30
Swin Transformer	99.11%	99.11%	0.091	0.092	30
Custom CNN	99.08%	98.47%	0.066	0.121	30
EfficientNetB4	99.41%	99.61%	0.060	0.080	30
ResNet101	98.82%	99.21%	0.126	0.104	30
Xception	95.12%	97.26%	0.296	0.249	30

Based on these outcomes, it is evident that both custom and fine-tuned models significantly contribute to vital brain tumor classification. The results indicate that CNN-based architectures remain reliable, while transfer learning approaches, especially EfficientNetB4 and Swin Transformer, excel in extracting discriminating features from medical images. Noticeably, the accuracy comparison, summarized in Table II, highlights the strong classification capabilities of both lightweight CNNs and transformer-based or transfer-learned models. Here, Table II compares the results of various models executed in our system.

All models were implemented using TensorFlow and Keras in Python. Training and testing were performed on a Kaggle platform using a P100 GPU.

V. CONCLUSION

This paper categorizes brain tumors from MRI scans into four classes, providing a robust classification approach for medical diagnostics. Consequently, our approach employed a custom light CNN architecture with optimized transformer-based models, such as EfficientNetB0, EfficientNetB4, ResNet101, Xception, and Swin Transformer, for automated disorder detection. This ensured a powerful type track that defined tumor categories and achieved high accuracy. Moreover, EfficientNetB4 outperformed as the most promising transformer model of all, achieving the highest accuracy of 99.61%. On the other hand, the custom light CNN model attained an accuracy of 99.48%, which can address the crucial challenges in medical diagnostics. Moreover, we aim to develop the system by combining numerous models that can be employed in different environments with high accuracy in limited resources for other medical imaging tasks.

REFERENCES

[1] Cleveland Clinic, "Brain cancer & brain tumor," 2025. Accessed: 2025-01-13.

[2] National Brain Tumor Society, "Brain tumor facts," 2025. Accessed: 2025-01-13.

[3] World Health Organization, "Migraine and other headache disorders," 2024. Published 6March2024; Accessed: 2025-01-13.

[4] Mayo Clinic, "Brain tumor: Symptoms and causes," 2025. Accessed: 2025-01-13.

[5] J. Yang and Q. Long, "A modification of adaptive moment estimation (adam) for machine learning," *Journal of Industrial and Management Optimization*, vol. 20, no. 7, pp. 2516–2540, 2024.

[6] Q. Zhang, "A novel resnet101 model based on dense dilated convolution for image classification," *SN Applied Sciences*, vol. 4, no. 1, p. 9, 2022.

[7] F. Chollet, "Xception: Deep learning with depthwise separable convolutions," in *Proceedings of the IEEE conference on computer vision and pattern recognition*, pp. 1251–1258, 2017.

[8] Z. Liu, Y. Lin, Y. Cao, H. Hu, Y. Wei, Z. Zhang, S. Lin, and B. Guo, "Swin transformer: Hierarchical vision transformer using shifted windows," in *Proceedings of the IEEE/CVF international conference on computer vision*, pp. 10012–10022, 2021.

[9] X. Liu and Z. Wang, "Deep learning in medical image classification from mri-based brain tumor images," in *2024 IEEE 6th International Conference on Power, Intelligent Computing and Systems (ICPICS)*, pp. 840–844, 2024.

[10] M. Behzadpour, B. L. Ortiz, E. Azizi, and K. Wu, "Breast tumor classification using efficientnet deep learning model," *arXiv preprint arXiv:2411.17870*, 2024.

[11] T. Dudeja, S. K. Dubey, and A. K. Bhatt, "Ensembled efficientnetb3 architecture for multi-class classification of tumours in mri images," *Intelligent Decision Technologies*, vol. 17, no. 2, pp. 395–414, 2023.

[12] A. Ghosh, B. Soni, and U. Baruah, "Transfer learning-based deep feature extraction framework using fine-tuned efficientnet b7 for multiclass brain tumor classification," *Arabian Journal for Science and Engineering*, vol. 49, 12 2023.

[13] J. Sachdeva, V. Kumar, I. Gupta, N. Khandelwal, and C. Ahuja, "Segmentation, feature extraction, and multiclass brain tumor classification," *Journal of digital imaging*, vol. 26, 05 2013.

[14] K. N. Rao, O. I. Khalaf, V. Krishnasree, A. S. Kumar, D. M. Alsekait, S. S. Priyanka, A. S. Alattas, and D. S. AbdElminaam, "An efficient brain tumor detection and classification using pre-trained convolutional neural network models," *Heliyon*, vol. 10, no. 17, p. e36773, 2024.

[15] M. B. Bashir, A. M. Rahi, M. K. Jahan, and A. Al Shafi, "Custom lightweight cnn and data-efficient models for efficient and fast convergence in lung cancer classification," in *2024 27th International Conference on Computer and Information Technology (ICCIT)*, pp. 477–481, 2024.

[16] N. Noreen, S. Palaniappan, A. Qayyum, I. Ahmad, and M. O. Alassafi, "Brain tumor classification based on fine-tuned models and the ensemble method.," *Computers, Materials & Continua*, vol. 67, no. 3, 2021.

[17] A. B. Abdusalomov, M. Mukhiddinov, and T. K. Whangbo, "Brain tumor detection based on deep learning approaches and magnetic resonance imaging," *Cancers*, vol. 15, no. 16, p. 4172, 2023.

[18] M. A. Khan and R. B. Z. Auvee, "Comparative analysis of resource-efficient cnn architectures for brain tumor classification," in *2024 27th International Conference on Computer and Information Technology (ICCIT)*, pp. 639–644, IEEE, 2024.

[19] M. Nickparvar, "Brain tumor mri dataset," 2021.

[20] A. Patil, M. Sanjana, M. Shilpa, R. Vaishnavi, and M. Priyadarshini, "Brain tumor detection and classification with one-hot encoding and efficientnetb0 using mri images," in *2024 5th International Conference on Image Processing and Capsule Networks (ICIPCN)*, pp. 84–90, 2024.